Bull. Mater. Sci., Vol. 31, No. 3, June 2008, pp. 501–505. © Indian Academy of Sciences.

Doped barium titanate nanoparticles

T K KUNDU*, A JANA[†] and P BARIK

Department of Physics, Siksha-Bhavan, Santiniketan 731 235, India
[†]Saldiha College, Saldiha, Bankura 721 312, India

Abstract. We have synthesized nickel (Ni) and iron (Fe) ion doped $BaTiO_3$ nanoparticles through a chemical route using polyvinyl alcohol (PVA). The concentration of dopant varies from 0 to 2 mole% in the specimens. The results from X-ray diffractograms and transmission electron micrographs show that the particle diameters in the specimen lie in the range 24–40 nm. It is seen that the dielectric permittivity in doped specimens is enhanced by an order of magnitude compared to undoped barium titanate ceramics. The dielectric permittivity shows maxima at 0·3 mole% doping of Fe ion and 0·6 mole% of Ni ion. The unusual dielectric behaviour of the specimens is explained in terms of the change in crystalline structure of the specimens.

Keywords. Nanostructured materials; nanoferroelectrics; $BaTiO_3$.

1. Introduction

Barium titanate (BT) has become increasingly important in the electro-ceramic industry, because of its ferroelectric, piezoelectric and thermoelectric properties (Phule and Risbud 1990). Also it has been widely studied due to its important applications in nonlinear optics (Shih *et al* 1994; Fu and Bellaiche 2003; Luo *et al* 2003), multilayer ceramic capacitors (MLCC), transducers, actuators, ferroelectric random access memories (FRAM) etc (Mathews *et al* 1997; Scott 1998; Park *et al* 1999). With the miniaturization of electronic devices, it is both scientifically interesting and technologically challenging to synthesize and characterize an ultrafine, preferably nanosized, barium titanate powders. Bulk $BaTiO_3$ has the classical ABO_3 (Ba^{2+} as A and Ti^{4+} as B) perovskite structure. Above the Curie temperature, $T_C \sim 130$°C (Jaffe *et al* 1971; Kwei *et al* 1993), it has a centro symmetric cubic crystal (*c*) structure (P_{m3m} space) with A at the corners, B at the centre, and the O^{2-} at the face centres. The ferroelectric properties of BT can be efficiently controlled by doping with different elements (Jona and Shirane 1993). It has been known that a high dielectric constant and good temperature stability can be achieved through addition of dopants. It is reported that the TiO_6 octahedra are disturbed with B-site doping resulting in broadening of the transition at T_C (Hennings *et al* 1982). It was shown that room temperature crystallographic structure of manganese doped $BaTiO_3$ ceramics, sintered at 1400°C in air, changes from tetragonal to hexagonal between 0·5 and 1·7 mole% of manganese (Langhammer *et al* 2000). As a driving force of the transformation from the cubic to the hexagonal crystal structure, the influence of the Jahn–Teller distortion is proposed. The grain sizes in those cases were in the range of micrometer. In this article, we report structural analysis and dielectric properties of Fe and Ni ion doped $BaTiO_3$ nanoparticles. Polyvinyl alcohol (PVA) has been used to encapsulate such crystallites.

2. Experimental

The compositions of the specimens can be represented by a general formula, $Ba(Ti_{1-z}X_z)O_3$, where X is Fe and Ni with $z = 0{\cdot}03$, 0·06, 0·1, 0·16 and 0·2. The specimens were prepared by a modified sol–gel route. The polymer template in Ba^{2+} and Fe/Ni doped Ti^{4+} cations arranged via PVA molecules was obtained by dispersing barium acetate, tetraisopropyle orthotitanate ($C_{12}H_{28}O_4Ti$) and $FeCl_3$/$Ni(NO_3)$ in PVA as follows.

First of all, a solution of ethyl alcohol and acetic acid in the volume ratio of 75 : 25 was prepared. Weighted amount of tetraisopropyl orthotitanate was hydrolyzed in that solution and the mixture (A) was stirred for 2 h. Aqueous solution of barium acetate (1·07 M) was poured into the first solution and the resulting mixture (B) was stirred for another 1 h. The solution B was clear and transparent. In the next stage, aqueous solution of ferric chloride (0·043 M)/ nickel nitrate (0·429 M) was added to the precursor B. Finally PVA (3 g/dl) was added to this solution drop-wise in a 5 : 2 ratio. As reported in the case of synthesizing a similar precursor for lead zirconate titanate or barium titanate or CrO_2 nanoceramic (Fang *et al* 1993; Jana *et al* 2004), active OH^- groups in PVA molecule absorb Ba^{2+}, Ti^{4+} and Fe^{2+}/Ni^{2+} cations over the molecular PVA surfaces in a specific template structure. Several processes of hydrolysis and polycondensation result in a polymer gel at room temperature. The gel was dried (in oven at 70°C for 24 h) and calcined at 750°C to crystallize the $BaTiO_3$ phase.

*Author for correspondence (tkkundu1968@yahoo.com)

Crystal structures were investigated using powder X-ray diffractometer (model PW1710) with filtered CuKα radiation of wavelength, $\lambda = 0{\cdot}15405$ nm. The calcined powders were isostatically pressed into pellets under pressure of 5 bars for 5 min. The pellets were sintered at 1000°C for 2 h for the measurement of dielectric permittivity. The capacitance of the sample was measured over the temperature range 300–473 K by using a LCR meter (Agilent-4284A). We have measured the density of the sintered material by Archimedes principle. Acetone was used as the solvent. The density of the specimens was around 5·2 g/cc. The reported value of the density of $BaTiO_3$ was found to be in the range 5·7 to 5·9 g/cc.

3. Iron ion doped $BaTiO_3$ nanoparticles

Figure 1 shows the XRD patterns of Fe ion doped $BaTiO_3$ specimens with pure BT derived by heating these polymer precursors at 750°C for 2 h in air. The peaks are indexed and the phase of tetragonal $BaTiO_3$ is identified. Figure 2 shows a typical transmission electron micrograph of the specimen doped with 0·3 mole% Fe^{3+}. Average grain sizes in the specimens lie in the range 29–40 nm. The PVA molecules absorb Ba^{2+}, Ti^{4+} and Fe^{3+} cations over the molecular PVA surfaces in a specific template structure. It is observed that the particle size in undoped BT increases from 29–40 nm due to sintering. Similarly in doped specimen 4, it increases from 39–49 nm. So, the grain sizes in the sintered specimen still lie in the range of nm whereas the grain size of the crystallites grows up to a few micrometers with conventional methods.

We have measured the dielectric property of the samples with variation of temperature at different frequencies. Figure 3 shows the variation of dielectric permittivity of doped and pure BT samples at 100 KHz. It is seen that the dielectric permittivity in doped specimens is enhanced compared to that of undoped $BaTiO_3$ ceramics. The Curie temperature strongly depends upon the dopant concentration and decreases with the increase of mole% of dopant. The dielectric permittivity of these samples is quite close to the values of BT nanoparticles as reported earlier, but lower than the values of BT having micron sized grain. It is reported that the value of dielectric constant is around

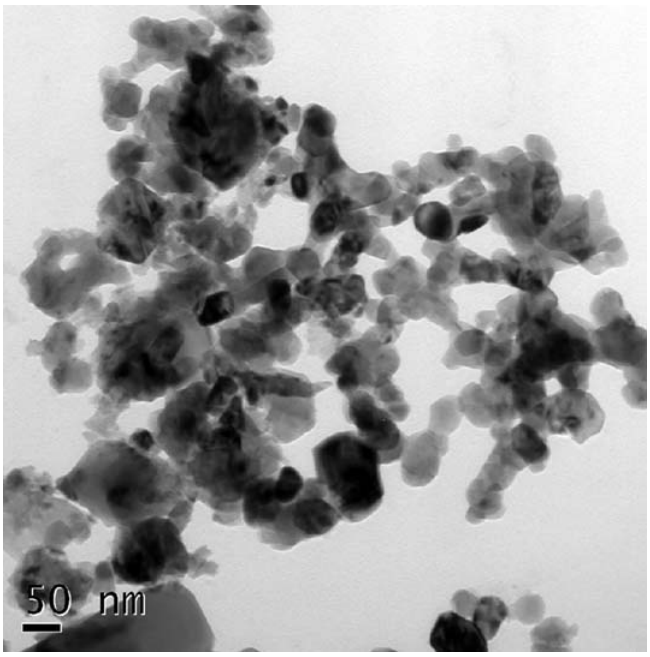

Figure 2. Transmission electron micrograph for 0·3 mole% Fe ion doped $BaTiO_3$.

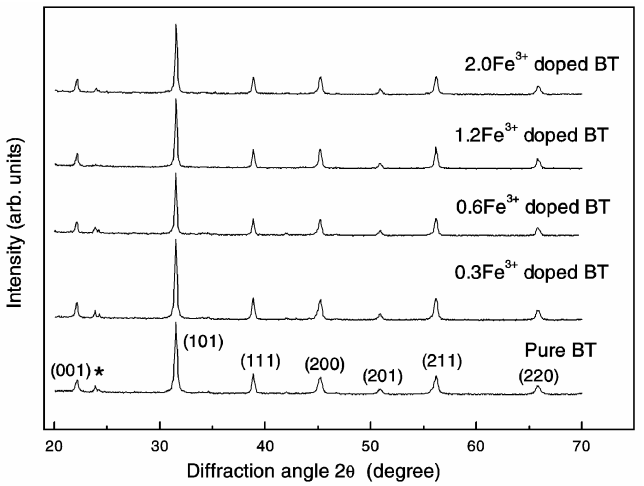

Figure 1. XRD pattern of undoped and Fe ion doped $BaTiO_3$ calcined at 750°C for 2 h.

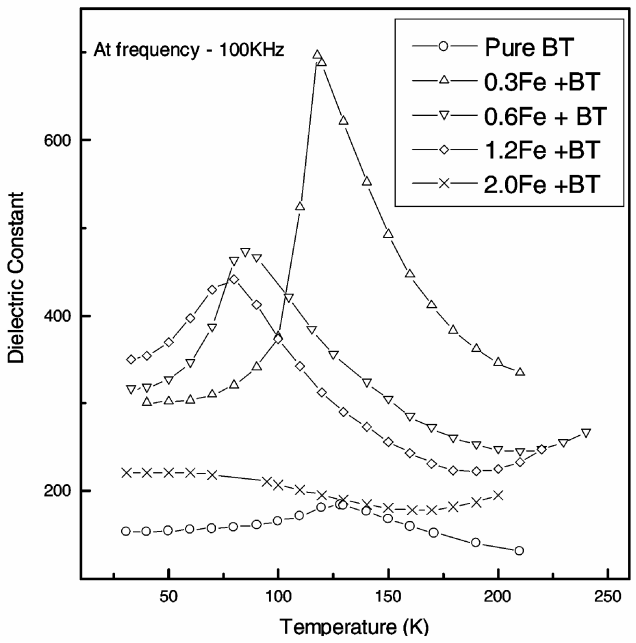

Figure 3. Variation of dielectric constant with temperature (at 100 kHz) of undoped and doped (Fe) specimens.

230 for specimens with grain size, 25 nm (Frey and Payne 1993) and according to Park (Park *et al* 2004), it is 700 having a grain size of 40 nm. It is also seen that the dielectric loss of all the specimens is < 1. We have also verified the Curie–Weiss law

$$1/\varepsilon = (T - T_0)/C.$$

With least square fitting it is found that the value of Curie–Weiss temperature (T_0) is 108, 68, 50 and 30 for 0·3, 0·6, 1·2 and 2 mole%, respectively. Also Curie constant (C) varied from $1{\cdot}66 \times 10^5$ °C–$9{\cdot}37 \times 10^5$ °C (Jana *et al* 2005). The deviation from the law is seen for the specimen doped with 2 mole% Fe^{3+}.

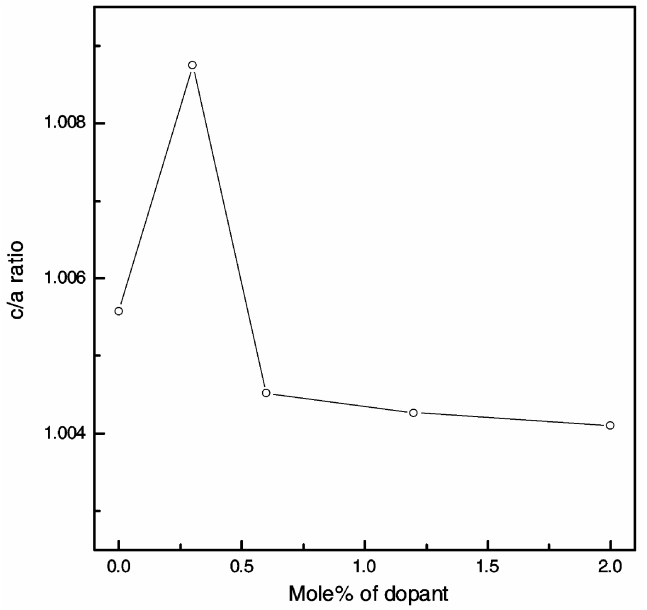

Figure 4. Variation of *c*/*a* ratio with mole% of Fe dopant.

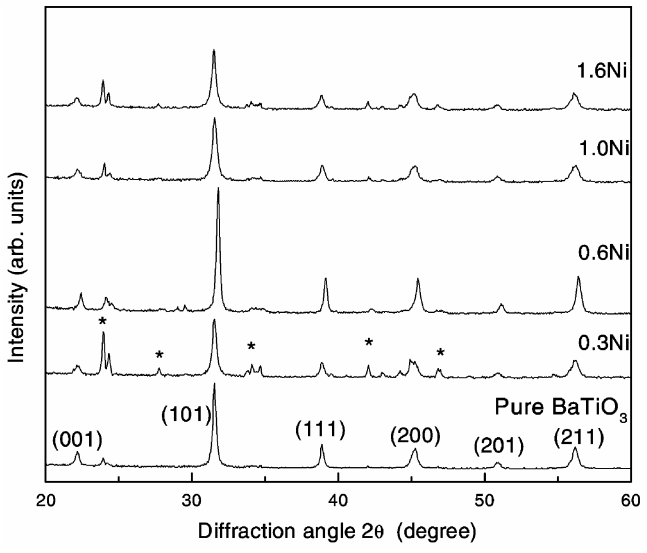

Figure 5. XRD pattern of undoped and Ni ion doped BT.

Previous reports show that the TiO_6 octahedra are disturbed with B-site doping resulting in a broadening of the transition at T_c (Hennings *et al* 1982). Specifically doping with 3d transition elements in BT stabilizes a different structural configuration in the system (Langhammer *et al* 2000). The composition dependence of T_c in μm sized BT was reported earlier (Jing *et al* 1998, 2003). The dielec-

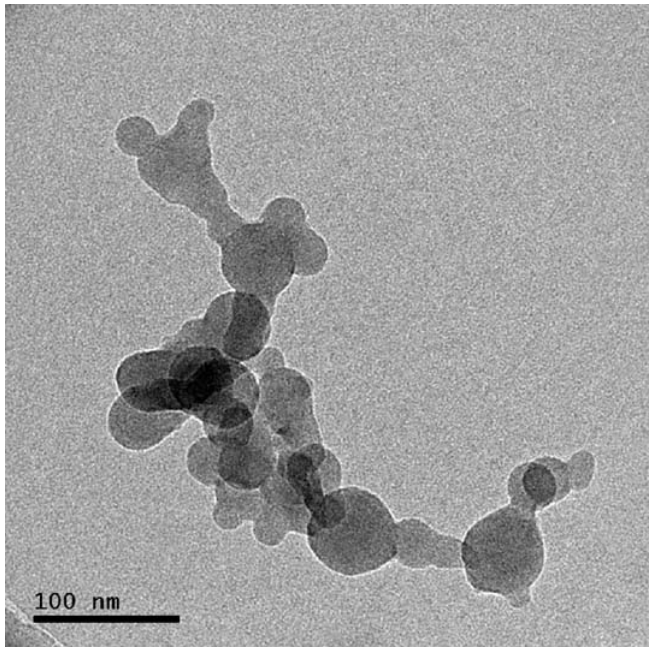

Figure 6. Transmission electron micrograph for 0·6 mole% Ni ion doped BT.

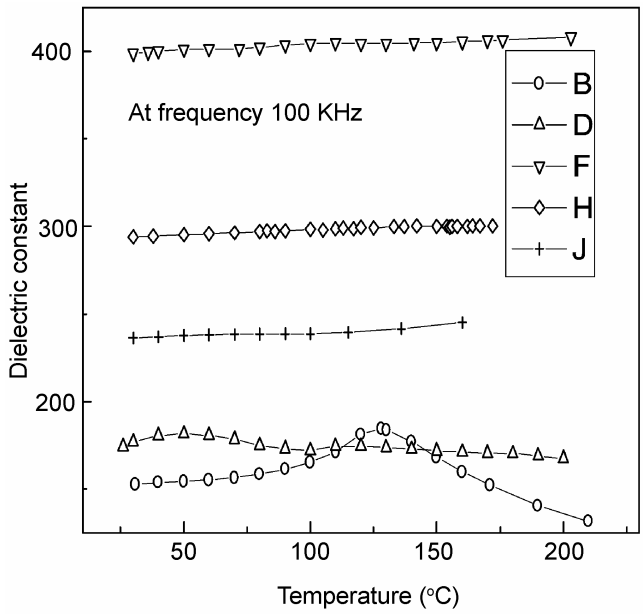

Figure 7. Variation of dielectric constant with temperature (at 100 kHz) of undoped and doped (Ni) specimens.

tric behaviour in those cases was explained in terms of the change in crystalline structure of doped BT specimens. A detailed analysis on the crystalline structure of the specimens is required to draw a similar conclusion in the present case, which is discussed later. Here, an important observation is that the dielectric permittivity maximum (ε_m) is highest in the specimen containing 0·3 mole% dopant. By using Rietveld method of analysis it was seen that c/a ratio is maximum (1·0087) at 0·3 mole% doped BT. Also a quality factor (GOF) approaching 1 (0·5–1·4) was obtained. Figure 4 shows the variation of c/a ratio with mole % of dopant. Thus, the variation of ε_m with composition can be explained in terms of change in lattice parameters 'c' and 'a' of the specimens.

4. Nickel ion doped $BaTiO_3$ nanoparticles

Here, Ti ions in $BaTiO_3$ were replaced by Ni ions. Mole % of Ni was 0·3, 0·6, 1·0 and 1·6. In figure 5, we have compared the XRD patterns of Ni doped and undoped $BaTiO_3$ samples derived by heating at 750°C for 2 h in air. The peaks are successfully indexed with the tetragonal structure of $BaTiO_3$. Figure 6 shows a typical electron micrograph of 0·6 mole% Ni^{2+} doped $BaTiO_3$. Particle sizes in the specimens lie in the range of 24–35 nm. The polymer precursor can very efficiently adjust the size of the grain as it serves as a surfactant to encapsulate the cationic species in divided groups during the reaction.

The dielectric properties of the samples were measured at different frequencies ranging from 1 kHz–1 MHz.

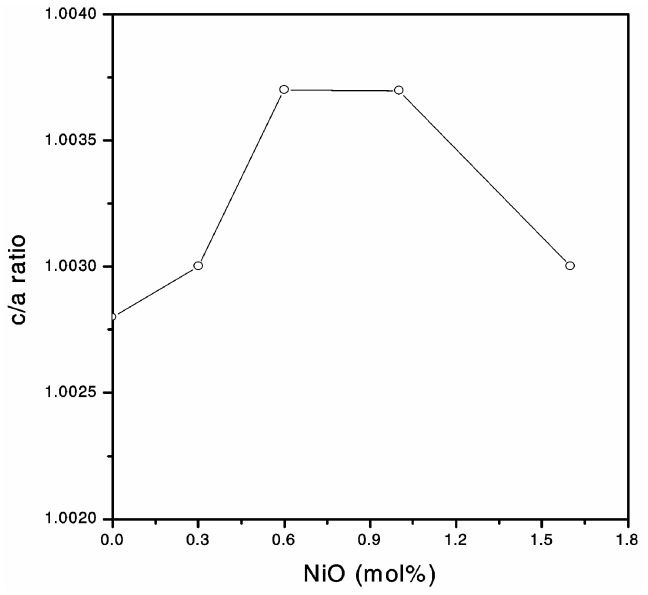

Figure 8. Variation of c/a ratio with the concentration of Ni ions.

Figure 7 compares the variation of permittivity of the specimens across the temperature at a frequency of 100 kHz. It is seen that the doped specimens possess higher dielectric constant than undoped ones. Room temperature dielectric permittivity is maximum at a dopant concentration of 0·6 mole%. It was reported earlier that the dielectric constant depends upon particle sizes in the specimens (Uchino *et al* 1989; Fang *et al* 1993). Normally, it decreases with the decrease of particle diameter. But here, average particle diameter in pure BT and 0·6 mole% Ni doped BT is 24 nm and 25 nm, respectively. Thus the present enhancement of ε did not result due to change in particle diameter. It is also seen that this effect is not caused due to space charge polarization (Jana and Kundu 2007).

During re-oxidation step for the processing of MLC, a small amount of NiO may dissolve into $BaTiO_3$. This causes a modification of the defect chemistry of the doped BT. Few reports are available on this issue where the microstructural changes in NiO doped micron sized BT are discussed (Tzing and Tsuan 1999; Tzing *et al* 1999; Albertsen 2004). The influence of Ni^{2+} ions on the crystal structure of micron sized BT was also investigated (Buscaglia *et al* 2000). The results were explained in terms of the change in crystalline structure of the specimens. An analysis on the crystalline structure of the specimens is required to draw a similar conclusion in the present case. We have calculated the lattice parameters 'a' and 'c' using Rietveld's powder structure refinement method. Figure 8 shows the variation of c/a ratio with Ni concentration. The parameter 'c' initially increases with the increase of dopant concentration and has a value of 0·4007 nm at 0·6 mole% of NiO. Later, it decreases with further increase of dopant concentration. Thus the variation of ε_m with composition can be explained in terms of the change in lattice parameters of the specimens.

5. Conclusions

Nanosized $BaTiO_3$ doped with transition metal ion like Fe/Ni were synthesized using chemical route. The concentration of dopant varies from 0–2 mole%. The particle diameters lie in the range 24–40 nm. The polymer precursor can very efficiently adjust the size of the grain as it serves as a surfactant to encapsulate the cationic species in divided groups during the reaction. Dielectric constant of doped $BaTiO_3$ specimens is higher than undoped ones. The dielectric permittivity shows maxima in the specimen containing 0·3 mole% of Fe^{3+} ion. The ferroelectric–paraelectric phase transition temperature (T_c) shifted to lower values with increase in Fe^{3+} concentration. In certain mole% of Ni^{2+}, the c/a ratio, as a result of the dielectric constant gets maximum. The dielectric results are explained in terms of change in lattice parameters (c/a) in the specimens.

Acknowledgement

The work was supported by a grant from the Nano Science and Technology Initiative of the Department of Science and Technology, New Delhi.

References

Albertsen K 2004 *J. Euro. Ceram. Soc.* **24** 1883
Buscaglia M T, Buscaglia V, Viviani M, Nanni P and Hanuskova M 2000 *J. Euro. Ceram. Soc.* **20** 1997
Fang T T, Hseih H L and Shiau F S 1993 *J. Am. Ceram. Soc.* **76** 1205
Frey M H and Payne D A 1993 *Appl. Phys. Lett.* **63** 2753
Fu H and Bellaiche L 2003 *Phys. Rev. Lett.* **91** 054402
Hennings D, Schnell A and Simon G 1982 *J. Am. Ceram. Soc.* **65** 135
Jaffe B, Cook W R and Jaffe H 1971 *Piezoelectric ceramics* (London: Academic Press)
Jana A and Kundu T K 2007 *Mater. Lett.* **61** 1544
Jana A, Ram S and Kundu T K 2004 *Indian J. Phys.* **A78** 97
Jana A, Kundu T K, Pradhan S K and Chakrabarty D 2005 *J. Appl. Phys.* **97** 044311
Jing Z, Ang C, Yu Z, Vilarinho P M and Bapista J L 1998 *J. Appl. Phys.* **84** 983
Jing Z, Yu Z and Ang C 2003 *J. Mater. Sci.* **38** 1057
Jona F and Shirane G 1993 *Ferroelectric crystal* (New York: Dover)
Kwei G H, Lawson A C, Billinge S J L and Cheong S W 1993 *J. Phys. Chem.* **97** 2368
Langhammer H T, Muller T, Felgner K and Abicht H 2000 *J. Am. Ceram. Soc.* **83** 605
Luo Y *et al* 2003 *Appl. Phys. Lett.* **83** 440
Mathews S, Ramesh R, Venkatesan T and Benedetto J 1997 *Science* **276** 238
Park B H, Kang B S, Bu S D, Noh T W, Lee J and Jo W 1999 *Nature* **401** 682
Park M B, Cho N H, Kim C D and Lee S K 2004 *J. Am. Ceram. Soc.* **87** 510
Phule P P and Risbud S H 1990 *J. Mater. Sci.* **25** 1169
Scott J F 1998 *Ferroelectr. Rev.* **1** 1
Shih W Y, Shih W H and Aksay I A 1994 *Phys. Rev.* **B50** 15575
Tzing W H, Tsuan W H and Lin H L 1999 *Ceram. Int.* **25** 425
Tzing W H and Tsuan W H 1999 *Ceram. Int.* **25** 69
Uchino K, Sadanaga E and Hirose T 1989 *J. Am. Ceram. Soc.* **72** 1555